Technology and Health Care 24 (2016) S795–S801
DOI 10.3233/THC-161212
IOS Press

Discrimination of motor imagery tasks via information flow pattern of brain connectivity

Shuang Liang[a], Kup-Sze Choi[b], Jing Qin[c,*], Qiong Wang[a], Wai-Man Pang[d] and Pheng-Ann Heng[e]
[a]*Shenzhen College of Advanced Technology, University of Chinese Academy of Sciences, Shenzhen, Guangdong, China*
[b]*School of Nursing, The Hong Kong Polytechnic University, Hung Hom, Hong Kong, China*
[c]*Centre for Smart Health, School of Nursing, The Hong Kong Polytechnic University, Hone Kong, China*
[d]*Department of Computer Science, Caritas Institute of Higher Education, Tseung Kwan O, Hong Kong, China*
[e]*Department of Computer Science and Engineering, The Chinese University of Hong Kong, Shatin, Hong Kong, China*

Abstract.
BACKGROUND: The effective connectivity refers explicitly to the influence that one neural system exerts over another in frequency domain. To investigate the propagation of neuronal activity in certain frequency can help us reveal the mechanisms of information processing by brain.
OBJECTIVE: This study investigates the detection of effective connectivity and analyzes the complex brain network connection mode associated with motor imagery (MI) tasks.
METHODS: The effective connectivity among the primary motor area is firstly explored using partial directed coherence (PDC) combined with multivariate empirical mode decomposition (MEMD) based on electroencephalography (EEG) data. Then a new approach is proposed to analyze the connection mode of the complex brain network via the information flow pattern.
RESULTS: Our results demonstrate that significant effective connectivity exists in the bilateral hemisphere during the tasks, regardless of the left-/right-hand MI tasks. Furthermore, the out-in rate results of the information flow reveal the existence of the contralateral lateralization. The classification performance of left-/right-hand MI tasks can be improved by careful selection of intrinsic mode functions (IMFs).
CONCLUSION: The proposed method can provide efficient features for the detection of MI tasks and has great potential to be applied in brain computer interface (BCI).

Keywords: Electroencephalogram (EEG), information flow pattern, multivariate empirical mode decomposition (MEMD), effective connectivity, motor imagery (MI)

1. Introduction

Brain connectivity analysis aims at describing the interaction between cortical regions by detecting the direction and strength of the information flow in these regions. There are two kinds of brain connec-

*Corresponding author: Jing Qin, Centre for Smart Health, School of Nursing, The Hong Kong Polytechnic University, Hone Kong, China. Tel.: 852 2766 6424 (O); Fax: 852 2364 9663 (O); E-maul: harry.qin@polyu.edu.hk.

tivity: functional connectivity and effective connectivity. The functional connectivity is defined as the statistical dependency and the temporal correlation between spatially remote neurophysiological events. The effective connectivity refers explicitly to the influence that one neural system exerts over another by analyzing the characteristics of frequency domains of the two systems [1]. This paper focuses on effective connectivity, as it has been verified that useful information in the brain signals is often coded in frequency. In this regard, to investigate the propagation of neuronal activity in certain frequency can help us reveal the mechanisms of information processing by brain.

However, accurate detection of effective connectivity and analysis of the complex brain network connection mode based on the detected effective connectivity remain challenging. The main challenge of the detection of effective connectivity is that the measured signals have power spectra consisting of numerous broad peaks in different frequency bands. To solve this problem, the recently proposed multivariate empirical mode decomposition (MEMD) method is utilized to decompose multichannel signals into a series of intrinsic oscillatory components called intrinsic mode functions (IMFs) through a sifting process. Due to precise separation of co-existing time scales, IMFs associated with diverse frequency bands can be used to investigate a causal effect between the signals. Compared with existing methods, such as bandpass filtering, short-time Fourier transform, wavelet transform, and Hilbert transform, which apply the time-frequency transformation to inappropriately decompose nonlinear and non-stationary EEG signal into a set of narrow-band signals [5], MEMD can make use of the multivariate data without the limitation of dealing with bivariate time series and break down a signal without leaving the time domain [6].

On the other hand, the common methods use graph theory algorithm to compute the various parameters in order to understand the original complex network connection mode. However, there is no widely accepted method for determining the threshold value when transforming the network model to the graph model. A new method is proposed based on the information flow to analyze the brain network. For the construction of the brain network, first MEMD is utilized to extract different frequency components from EEG signals. Then, effective connectivity is detected based on the different frequency components using partial directed coherence (PDC) [4]. The proposed method can simplify the complex network model, helping us to explore brain mechanism. In this paper, this method is employed to discriminate different motor imagery tasks, which has great potentials to be used in brain-computer interface (BCI) applications.

2. Materials and methods

2.1. EEG dataset of motor imagery tasks

The BCI competition IV dataset 2a was employed in our study [7]. The data of nine subjects were acquired from twenty-two Ag/AgCl electrodes sampled at 250 Hz and bandpass filtered between 0.5 Hz and 100 Hz. The electrode positions are shown in Fig. 1 (left). Each subject performed four MI tasks (left hand, right hand, foot and tongue) according to the experimental paradigm, as shown in Fig. 1 (right). At the beginning of each experiment, a fixation cross appeared on the black screen with a short acoustic warning tone. After 2 s, a cue in the form of an arrow appeared for prompting the subjects to take the desired MI tasks until the fixation cross disappeared from the screen at $t = 6$ s. A short break followed when the screen was black again. This study focuses on the data of left-/right-hand MI tasks. As a former study revealed that the most reactive frequency components of left-/right-hand MI varied between 8Hz and 30 Hz [8], this paper further bandpass filtered the EEG data for the following analysis.

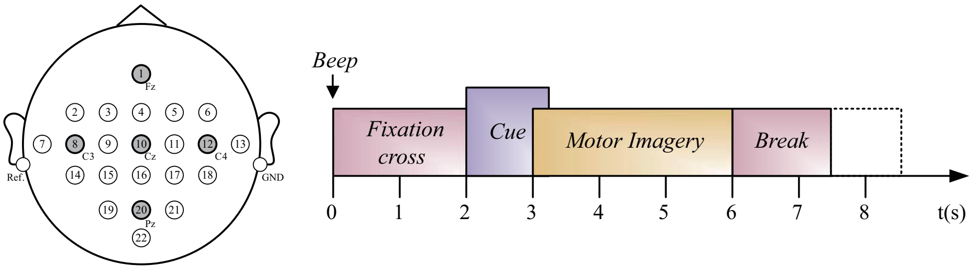

Fig. 1. Left: the electrode positions; right: the experimental paradigm used in [7].

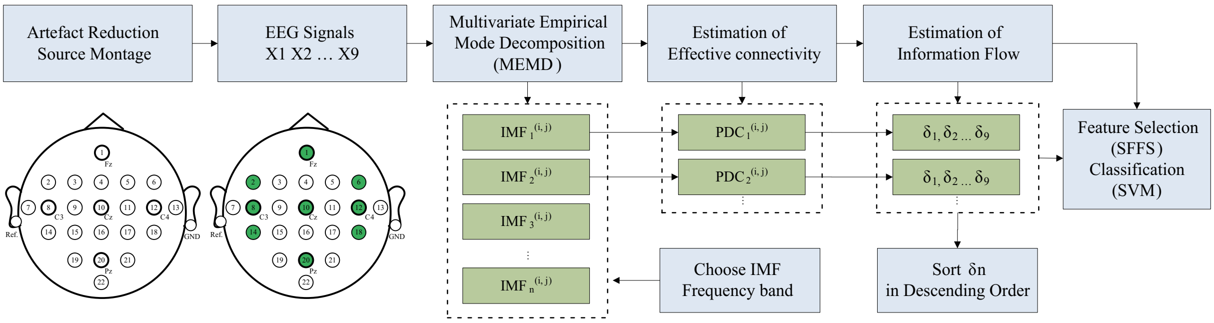

Fig. 2. The workflow of the proposed method.

2.2. Workflow of the proposed method

Figure 2 shows the workflow of the proposed method, including the acquisition, the pre-processing and the analysis of EEG data. The source EEG signals were reduced from 22 to 9 channels as X1, X2…X9. Then, as mentioned, the selected signals of the 9 channels were filtered by 8–30 Hz bandpass. Then the newly proposed MEMD is employed to extract different frequency components from the signals, which were fed into the PDC to more accurately detect the causality connectivity between the electrodes. According to causality connectivity, we further analyzed the information flow pattern in the connections was analyzed further. To estimate the contributions of a specific brain location to a specific MI task via the information flow pattern, the out-in rate at each electrode was computed and sorted in a descending order. After feature selection on these out-in rates using SFFS, SVM was applied to train a classifier and classify the testing data.

2.3. Decomposition of EEG signal

The MEMD, a generic extension of the standard EMD, has been recently proposed by Rehman and Mandic [6]. The main advantage of MEMD is that it can more effectively decompose a signal to components with different frequency than traditional standard EMD. To the end, MEMD was employed to decompose the EEG signals. The details of the MEMD algorithm for n-dimensional signals $\{X(t)\}_{t=1}^{T} = \{x_1(t), x_2(t), ..., x_N(t)\}$ decomposition can be summarized as follows:

1. Select a point set for sampling on a $(N-1)$ sphere.
2. Calculate a projection $\{p^{\theta_k}(t)\}_{t=1}^{T}$ of the original signal $\{X(t)\}_{t=1}^{T}$ along the direction vector d^{θ_k}, giving θ^k as the direction angles on the $(N-1)$ sphere. For all k direction vectors, calculate the set of projections $\{p^{\theta_k}(t)\}_{k=1}^{K}$.

3. Identify the time instants $t_j^{\theta^k}$ corresponding to the maxima of the set of projected signals $\left\{p^{\theta_k}(t)\right\}_{k=1}^{K}$.
4. Obtain multivariate envelopes curves $\left\{e^{\theta_k}(t)\right\}_{k=1}^{K}$ by interpolating $\left[t_j^{\theta_k}, X\left(t_j^{\theta_k}\right)\right]$.
5. Calculate the local mean $m(t) = 1/K \sum_{k=1}^{K} e^{\theta_k}(t)$ of the envelopes curves for a set of K direction vectors.
6. Subtract the local mean from $X(t)$,$c_i(t) = X(t) - m(t)$ (i is an order of IMF). Test if $c_i(t)$ can fulfill the stoppage criterion for a multivariate IMF. If yes, repeat the above procedure to $X(t) - c_i(t)$, otherwise apply the procedure to $c_i(t)$.

At the end of the decomposition, the original signal $\{X(t)\}_{t=1}^{T}$ can be represented as

$$X(t) = \sum_{i=1}^{M} c_i(t) + r(t), \tag{1}$$

where M is the number of IMFs, $c_i(t)$ is the ith IMF, and $r(t)$ is the remaining residue.

2.4. Detection of the causality connectivity with PDC

The causality connectivity between the electrodes was detected using PDC based on the decomposed signals. Given a set $\{X(t)\}_{t=1}^{T} = \{x_1(t), x_2(t), ..., x_N(t)\}$ of simultaneously observed multichannel EEG signals described by the following multivariate autoregressive (MVAR) process:

$$\sum_{r=1}^{p} \Lambda(r) X(t-r) = E(t) \text{ with } \Lambda(0) = I, \tag{2}$$

where $E(t)$ is a vector of multivariate zero-mean uncorrelated white noise process and $\Lambda(r)$ is the $N \times N$ matrices of model coefficients, the dimension p in the model can be estimated using the Akaike criterion, while the values of coefficients in Eq. (2) can be obtained by the Nuttall-Strand method, which is reported to be the best one among multivariate autoregressive estimators [9]. In order to investigate the spectral properties of the examined process, Eq. (2) is transformed to the frequency domain. $\Lambda(f) X(f) = E(f)$, where $\Lambda(f) = \sum\limits_{r=0}^{p} \Lambda(r) e^{-j2\pi f \Delta t r}$ and Δt is the temporal interval between two samples. The PDC from $x_i(k)$ to $x_j(k)$ is then defined by:

$$\pi_{i \leftarrow j}^2(f) = \frac{|\Lambda_{ij}(f)|^2}{\sum\limits_{k=1}^{N} |\Lambda_{kj}(f)|^2} \tag{3}$$

The PDC provides a measure for calculating the direct influence of x_j to x_i via the comparison of the linear influence of x_j on x_i at the frequency f with the influence of x_i on the other variables.

After estimation of the PDC, null hypothesis of $|\pi_{i \leftarrow j}(f)| = 0$ tests can be performed for each frequency and each channel pair at 5%. It can be rejected if the estimated PDC exceeds a threshold value calculated by the Patnaik approximation of quantile thresholds, utilizing χ_v^2 distribution with non-integer v, which can be computed using the gamma function [10].

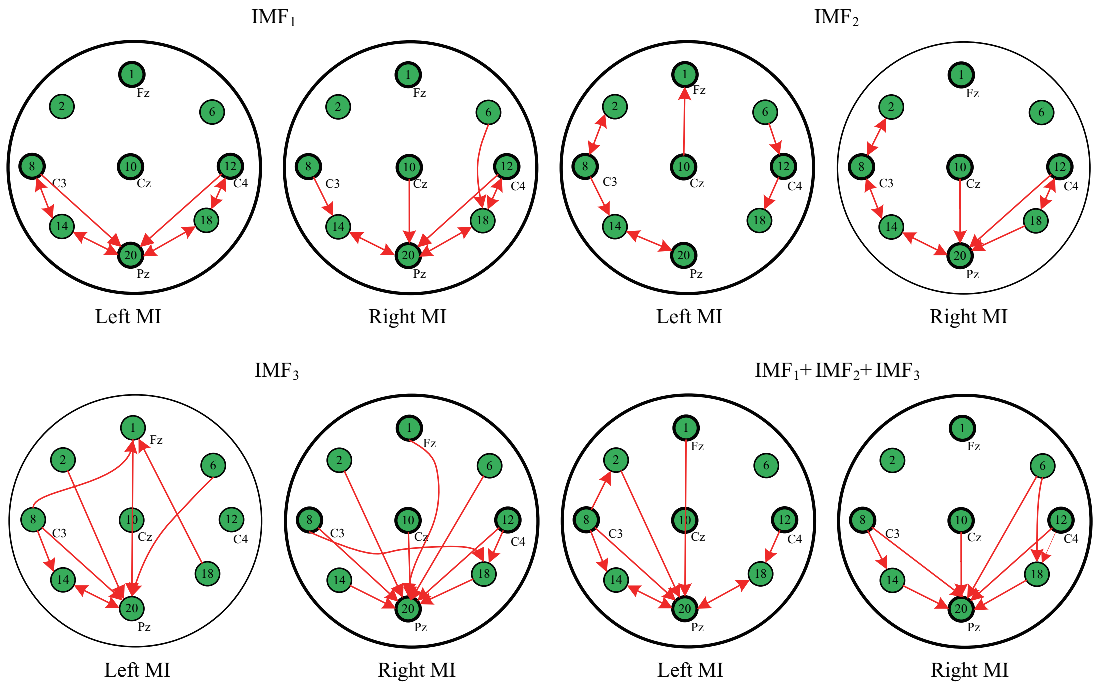

Fig. 3. The most ten significant effective connectivity during the left-hand motor imagery and right-hand motor imagery respectively, and the directional connectivity represented by the red arrows.

2.5. Estimation of information flow

Given channel k for instance, the input and output of information flow are defined as,

$$IN = \sum_{j=1}^{N} \pi_{k\leftarrow j}^{2}(f) \text{ and } OUT = \sum_{i=1}^{N} \pi_{i\leftarrow k}^{2}(f) \tag{4}$$

where IN represents the information flow from other channels into the channel k as the destination location, and OUT denotes the information flow sent by channel k as the source location. Then, it is defined that

$$\delta_k = \frac{OUT}{IN} = \frac{\sum_{i=1}^{N} \pi_{i\leftarrow k}^{2}(f)}{\sum_{j=1}^{N} \pi_{k\leftarrow j}^{2}(f)} \tag{5}$$

In addition, it means none or little information output when δ_k decreases towards zero, while the contributions of the brain localization in the processing of information flow become more significant with the increase of δ_k.

δ_k over different frequency bands was calculated. Then the δ_k was employed to train the SVM classifier. A 10×10 cross-validation procedure was applied to test the performance of the classifier, which may avoid over-fitting and enhance the generalization of classification results.

Table 1
The results of out-in rate at different locations in left-/right-hand MI tasks

Out-in	IMF_1		IMF_2		IMF_3	
rate	Left	Right	Left	Right	Left	Right
δ_1	0.99	0.97	1.01	1.04	1.10	1.13
δ_2	1.05	1.04	1.06	1.05	1.11	1.12
δ_3	1.06	1.05	1.06	1.09	1.12	1.13
δ_4	1.08	1.11	1.09	1.07	1.12	1.16
δ_5	1.02	1.02	1.06	1.06	1.15	1.14
δ_6	1.12	1.10	1.10	1.11	1.15	1.16
δ_7	1.01	1.05	1.05	1.04	1.08	1.09
δ_8	1.04	1.03	1.06	1.04	1.10	1.08
δ_9	0.94	0.95	0.98	0.97	1.05	1.03

Table 2
The classification results of left-/right-hand MI tasks (%)

	S_1	S_2	S_3	S_4	S_5	S_6	S_7	S_8	S_9	Mean
IMF_1	62.13	67.86	75.71	72.14	67.46	66.67	71.43	78.57	70.00	70.22
IMF_2	66.67	67.46	65.00	72.14	69.05	67.86	68.75	71.43	65.00	68.15
IMF_3	72.14	73.81	67.14	64.29	69.29	75.00	67.86	72.14	63.57	69.47
$IMF_1 + IMF_2 + IMF_3$	67.86	71.43	68.57	68.57	66.43	62.50	62.86	70.71	71.43	68.13

3. Results and discussion

3.1. Effective connectivity analysis

It is well known that hand movements activate primarily contralateral hemispheric areas. According to a recent study, lateralization occurred not only in the neural activity but also in the effective connectivity networks [11]. However, from the Fig. 3, our results showed that significant effective connectivity existed in the bilateral hemisphere (primary motor area, M1) during the hand MI tasks, regardless of the left/right-hand MI tasks. In addition, the results suggested that the effective connectivity networks could be changed across different frequency bands.

3.2. Analysis of information flow

Table 1 shows the average out-in rates of nine subjects with different IMF_n at different locations. The results of out-in rate with different IMF_n primarily showed that the significant contributions of the brain regions were found in contralateral hemispheric localization, regardless of the left-/right-hand MI tasks. δ_n represented the location of electrodes. In the Table 1, for IMF_1 and IMF_3, the right hemisphere is more active than the ipsilateral hemispheric during left-hand MI tasks, compared to that in the left hemisphere during right-hand tasks. However, our results showed the right hemispheric lateralization in the IMF_2 case. Since the IMF_n corresponds to different frequency bands, the out-in rate results of information flow from the brain localizations would be affected by them.

3.3. Classification results

Table 2 shows the classification results of left-/right-hand MI tasks in different frequency bands for all nine subjects. It is observed that the best classification results were alone with either IMF_1 or IMF_3 for most subjects, revealing that taking frequency into account could improve the classification performance.

4. Conclusion

This paper investigates the features of the effective connectivity networks in primary motor area during left-/right-hand MI tasks by means of PDC combined with MEMD. Experimental results evidence that significant effective connectivity exists in the bilateral hemisphere during the hand MI tasks. The out-in rates imply that the contralateral lateralization and right lateralization exist during left-/right-hand MI tasks. By calculating the out-in rates of different IMF_n, the classification performance of left-/right-hand MI tasks can be obviously improved. Future works include testing more activated locations instead of only nine electrodes, extending the current framework to multi-class classification and further investigating the information flow pattern in the effective connectivity networks during various MI tasks.

Acknowledgements

The work described in this paper was supported by National Basic Research Program of China, 973 Program (Project No. 2015CB351706), Research Grants Council of the Hong Kong Special Administrative Region, China (Project No. CUHK 412412), Research Grants Council of the Hong Kong SAR (PolyU5134/12E), Hong Kong Polytechnic University (G-UC93), and Shenzhen Basic Research Project (Project No. JCYJ20130402113127511), and a scholarship donated by Nelson Y.C Yu.

References

[1] Friston K J. Functional and effective connectivity: a review[J]. Brain connectivity. 2011, 1(1): 13-36.
[2] Kaminski M J, Blinowska K J. A new method of the description of the information flow in the brain structures[J]. Biological cybernetics. 1991, 65(2): 203-210.
[3] Baccalá L A, Sameshima K. Partial directed coherence: a new concept in neural structure determination[J]. Biological cybernetics. 2001, 84(6): 463-474.
[4] Gourévitch B, Le Bouquin-Jeannès R, Faucon G. Linear and nonlinear causality between signals: methods, examples and neurophysiological applications[J]. Biological cybernetics. 2006, 95(4): 349-369.
[5] Al-Fahoum A S, Al-Fraihat A A. Methods of EEG Signal Features Extraction Using Linear Analysis in Frequency and Time-Frequency Domains[J]. ISRN neuroscience. 2014.
[6] Rehman N, Mandic D P. Multivariate empirical mode decomposition[C]//Proceedings of The Royal Society of London A: Mathematical, Physical and Engineering Sciences. The Royal Society, 2009: rspa20090502.
[7] Tangermann M, Müller K R, Aertsen A, et al. Review of the BCI competition IV[J]. Frontiers in neuroscience. 2012, 6.
[8] Ramoser H, Muller-Gerking J, Pfurtscheller G. Optimal spatial filtering of single trial EEG during imagined hand movement[J]. Rehabilitation Engineering, IEEE Transactions on. 2000, 8(4): 441-446.
[9] Schlögl A. A comparison of multivariate autoregressive estimators[J]. Signal processing. 2006, 86(9): 2426-2429.
[10] Yasumasa TD, Antonio BL, Sameshima K. Connectivity inference between neural structures via partial directed coherence[J]. Journal of Applied Statistics. 2007, 34(10): 1259-1273.
[11] Gao Q, Duan X, Chen H. Evaluation of effective connectivity of motor areas during motor imagery and execution using conditional Granger causality[J]. Neuroimage. 2011, 54(2): 1280-1288.